

Impact of Urban Land-Use Change in Eastern China on the East Asian Subtropical Monsoon: A Numerical Study

YU Rong^{1,2} (余 荣), JIANG Zhihong^{1,2} (江志红), and ZHAI Panmao^{3*} (翟盘茂)

¹ Collaborative Innovation Center on Forecast and Evaluation of Meteorological Disasters and

Key Laboratory of Meteorological Disaster of Ministry of Education,

Nanjing University of Information Science & Technology, Nanjing 210044

² College of Atmospheric Science, Nanjing University of Information Science & Technology, Nanjing 210044

³ State Key Laboratory of Severe Weather, Chinese Academy of Meteorological Sciences, Beijing 100081

(Received August 25, 2015; in final form February 9, 2016)

ABSTRACT

The effect of urban land-use change in eastern China on the East Asian subtropical monsoon (EASTM) is investigated by using the Community Atmosphere Model version 5.1. Comparison of the results between the urban expansion and reference experiments shows that with the urban expansion, the land surface energy balance alters: surface net radiation and sensible heat fluxes enhance while the latent heat fluxes reduce. As a result, a significant increase in surface air temperature over eastern China is detected. The urban land-use change contributes to a change in the zonal land-sea temperature difference (LSTD), leading to a delay in the time when LSTD changes from positive to negative, and vice versa. Additionally, the onset and retreat dates of the EASTM are also delayed. Meanwhile, the rise in surface air temperature leads to formation of abnormal northerly air flows, which may be the reason for the slower northward movement of the EASTM and a more southward location of its northern boundary.

Key words: urban land-use change, the East Asian subtropical monsoon, northern boundary

Citation: Yu Rong, Jiang Zhihong, and Zhai Panmao, 2016: Impact of urban land-use change in eastern China on the East Asian subtropical monsoon: A numerical study. *J. Meteor. Res.*, **30**(2), 203–216, doi: 10.1007/s13351-016-5157-4.

1. Introduction

China is located in the East Asian monsoon region, which is divided into the subregions of East Asia and India. Further, the East Asian monsoon is demarcated into the South China Sea monsoon and the East Asian subtropical monsoon (EASTM) (Zhu et al., 1986; Ding et al., 2015). Studying the EASTM is important to the forecast of weather and climate in China. Abnormalities in both the intensity and scale of the EASTM can lead to severe weather and climatic disaster, which can cause (directly or indirectly) substantial socioeconomic damage. Owing to the special land-sea geographical distribution of East Asia, the thermal difference in this area is manifested not only meridionally but also zonally. Based on the large

body of research on the features of the EASTM's evolution, it is known that its onset is determined by the zonal land-sea thermal difference (LSTD) (He et al., 2007, 2008; Qi et al., 2008; Zhao et al., 2009). Meanwhile, large-scale urbanization can contribute to terrestrial heating anomalies over eastern China (Kalnay and Cai, 2003; Pitman et al., 2012; Christidis et al., 2013; Wu and Yang, 2013), and to some extent may cause changes in atmospheric thermal forcing (Li et al., 2011; Zhang et al., 2011) and variations in precipitation (Zhang et al., 2009; Ao et al., 2012; Deng et al., 2014b; Chen et al., 2015). As the onset of the EASTM is related to a reversal in the zonal LSTD, and a change in urban land use could lead to terrestrial heating anomalies, the latter may affect the onset of the EASTM.

Supported by the National Natural Science Foundation of China (41175080).

*Corresponding author: pmzhai@cma.gov.cn.

©The Chinese Meteorological Society and Springer-Verlag Berlin Heidelberg 2016

At the same time, a number of studies have examined the northern boundary of the East Asian summer monsoon (Wang and Lin, 2002; Wang et al., 2014). As the transition zone between the monsoon and non-monsoon zones, the northern boundary of the East Asian (subtropical) summer monsoon has a significant influence on the weather and climate (including extreme weather and climate events) in the eastern parts of Northwest China, North China, and Northeast China, especially over the Yellow River basin (Li et al., 2013a). The northerly march of the East Asian summer monsoon (or the EASTM) displays obvious interdecadal variability (Wang, 2001; Wang and Fan, 2013), with its zonal position showing a sudden northward jump in the mid 1960s and its intensity showing a jump in the late 1970s as well (Jiang et al., 2006). With consideration of precipitation, vector wind, and potential pseudo-equivalent temperature (θ_{se}), the northern boundary of the East Asian summer monsoon also shows obvious interdecadal variations (Hu and Qian, 2007). Furthermore, progress has been made in identifying the factors affecting the location of the northern boundary of the East Asian summer monsoon. There is a notable and persistent negative correlation between the surface sensible heat flux over the eastern arid region of Northwest China and the location of the northern boundary of the East Asian monsoon during May–September (Li et al., 2013b). Owing to the existence of the Tibetan Plateau, the intensity of southerly wind is enhanced, and as a result the location of the northern boundary of the East Asian summer monsoon reaches a more northern position (Tang et al., 2006). Be noted that the northern boundary of the East Asian summer monsoon is actually the same as that of the EASTM, so we will use the latter exclusively in the remaining text of this paper. Generally, the obvious interdecadal variability of the EASTM and its northern boundary is very likely to be influenced by surface thermal factors, such as sensible heat flux.

IPCC AR5 (2013) reported that anthropogenic land-cover change has a direct impact on the earth's radiation budget through a change in the surface albedo. It also has an influence on local climate

through modifications to the surface roughness, latent heat flux, and runoff, while it may have undesirable impacts on the atmospheric circulation and shifts of precipitation patterns. Studies on the possible impacts of large-scale urbanization in eastern China on the East Asian winter monsoon show that the East Asian winter monsoon would weaken while the winter monsoon in Northeast China would intensify (Chen and Zhang, 2013; Deng and Xu, 2014; Ma et al., 2015). The large-scale urban land-use change, which is a significant factor impacting land surface heating, has drawn considerable concern about its effects on climate change and seasonal variance of climate, but there have been few studies of its influences on large-scale monsoon circulation, especially the seasonal march of the EASTM. It is worthy of a further investigation on the effects of large-scale urban land-use change (ULUC) on variations of the EASTM.

In this study, based on the high-resolution Community Atmosphere Model version 5.1 (CAM5.1), the impact of ULUC in eastern China on the onset/retreat of the EASTM and its northern boundary as well as the possible mechanism involved, are investigated, by analyzing seven model simulation experiments over a 20-yr period with changed underlying land-use conditions. Following this introduction, we begin by describing the model and experimental design in Section 2. The simulation results, which cover the impact of ULUC on surface climate, the effects of urban land-use on the onset and retreat dates of the EASTM and its northern boundary, are analyzed in Section 3. Finally, Section 4 summarizes the key findings and provides further discussion.

2. Model and experimental design

2.1 Climate model

The global atmospheric general circulation model, CAM5.1 (Neale et al., 2010), of the Community Earth System Model version 1 (CESM1), of the National Center for Atmospheric Research (NCAR), was used in this study. It can couple with the Community Land Model (CLM), the sea-ice component (CICE), and the data ocean component (DOCN). For the boundary

conditions, the ocean and sea-ice data were from observations. The land component of CESM1.0.3, CLM4.0 (Oleson et al., 2010), contains a Community Land Model Urban (CLMU; Oleson et al., 2015) parameterization module, which includes parameters in three aspects: urban spatial scope, morphological features, and thermodynamic and radiative properties of building materials. In this study, CAM5.1 coupled with CLM4.0 was employed to study the impact of ULUC. Many studies have used this model to investigate the effects of urbanization (Oleson et al., 2008; Deng et al., 2014a; Ma et al., 2014), and the results suggest that CLM4.0 is an effective tool in this regard.

2.2 Experimental design

According to the latest records of the National Bureau of Statistics (2014), China's urbanization ratio increased from 36% in 2000 to 53% in 2012. To investigate the effect of large-scale urban expansion in eastern China (20° – 50° N, 100° – 125° E) on the EASTM, seven climate simulations were performed in the current study. The first is the reference experiment (referred to as NOURB), in which there is no urban land cover in eastern China; the urban land-use is changed to an all natural (without urban) land cover, i.e., the urban land cover fraction is set to zero (Fig. 1a). The

present run (PRURB) uses the default land cover (Fig. 1b), while five additional sensitivity runs involve increasing the urban area in each model grid box of eastern China by 1.5 (1.5URB), 2 (2.0URB), 3 (3.0URB), 4 (4.0URB), and 5 (5.0URB) times (Figs. 1c–g), respectively.

The CAM5.1 used in this study was set with a horizontal resolution of 0.9° latitude \times 1.25° longitude, and a hybrid vertical coordinate with 30 levels. The model was run with 1988–2007 monthly average SSTs, with annual variations (Hurrell et al., 2008), as its ocean surface boundary conditions. All experiments were integrated for 20 yr (from 1 January 1988 to 31 December 2007), with the first 5 years used for spin-up and only the last 15 years (1993–2007) of meteorological variables in the East Asian monsoon region stored (on a monthly basis) and analyzed.

2.3 Index definition

2.3.1 Onset and retreat of the EASTM

The onset of the tropical summer monsoon was based on the reversal of meridional LSTD, while the onset of the EASTM was dependent on the zonal LSTD (Qi et al., 2008). Thus, the onset of the EASTM is defined by the first pentad when the 850-hPa zon-

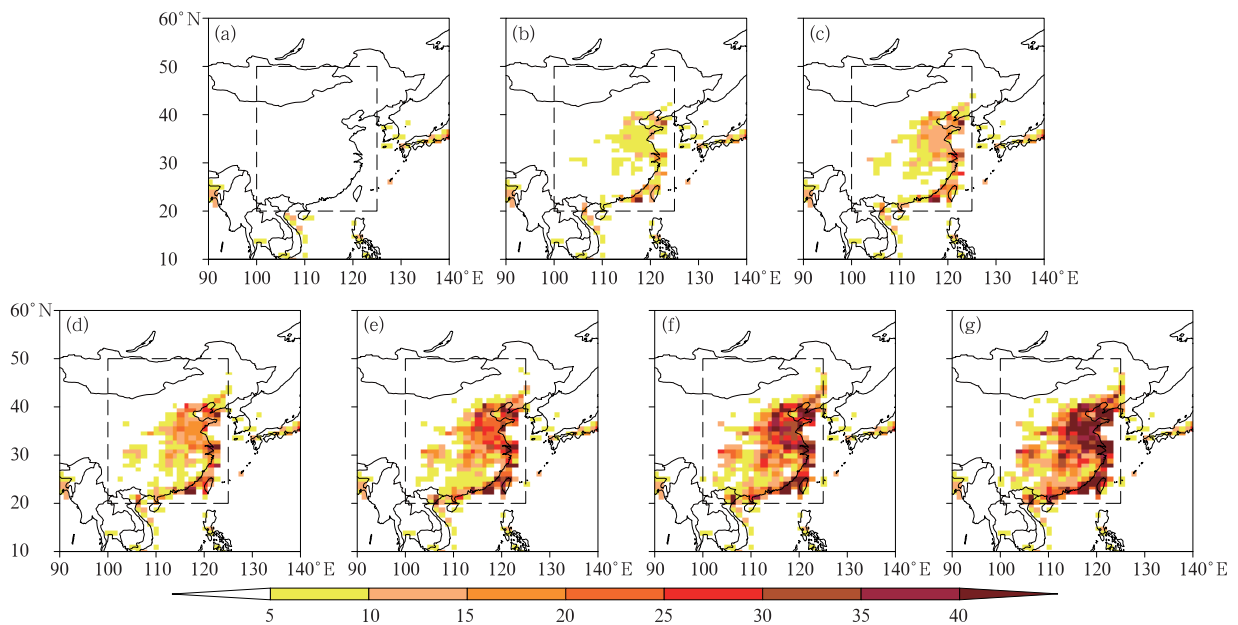


Fig. 1. Spatial distributions of the urban cover (%) over eastern China in the (a) NOURB, (b) PRURB, (c) 1.5URB, (d) 2.0URB, (e) 3.0URB, (f) 4.0URB, and (g) 5.0URB experimental runs. Eastern China is delineated by the dashed box; only the land cover within this box is altered to various degrees in the seven experiments.

al wind averaged over the subtropical area (27.5° – 32.5° N, 110° – 140° E), i.e., V , satisfies the following two criteria: (1) during the onset pentad, $V \geq 0 \text{ m s}^{-1}$; (2) during the onset pentad and the subsequent three pentads, $V > 0.5 \text{ m s}^{-1}$. Meanwhile, the retreat of the EASTM is defined by $V < 0 \text{ m s}^{-1}$. This definition has been used in Wang et al. (2004), and proved to be a good index.

2.3.2 Northern boundary of the EASTM

With consideration of precipitation, wind, and potential pseudo-equivalent temperature (θ_{se}), the northern boundary of the EASTM needs to satisfy the following three criteria (Hu and Qian, 2007): (1) the 850-hPa pentad-averaged wind should be southwesterly wind, that is, $U \geq 0 \text{ m s}^{-1}$ and $V \geq 0 \text{ m s}^{-1}$; (2) 850-hPa pentad-averaged $\theta_{se} \geq 340 \text{ K}$; and (3) pentad-averaged precipitation $P \geq 5 \text{ mm day}^{-1}$.

2.4 Model validation

The simulation results of PRNRB were compared with NCEP/NCAR reanalysis data to evaluate the model performance in simulating the April–August climate over East Asia. The NCEP/NCAR reanalysis data used include geopotential height, horizontal wind, and surface air temperature on a resolution of 2.5° latitude \times 2.5° longitude (Kalnay et al., 1996). The time period 1979–2007 was chosen for the evaluation.

Figure 2 shows that, for both PRNRB and NCEP/NCAR in April (Figs. 2a and 2f), the western Pacific subtropical high (WPSH) remains in the Indo-China Peninsula–South China Sea region, the geopotential height is low over the Bay of Bengal, and the Somali jet and cross-equatorial flows are absent; in May (Figs. 2b and 2g), the WPSH is stronger and slightly eastward, southwesterly flows prevail from the Indo-China Peninsula to the southern part of the South China Sea, and the Somali jet and cross-equatorial flows appear; in June (Figs. 2c and 2h), the East Asian cross-equatorial flows extend further northward, while the westerly wind in the Arabian Sea and Bay of Bengal intensifies; in July (Figs. 2d and 2i), the WPSH jumps northward and remains stable over the Yangtze and Huai River area; and in August (Figs. 2e and 2j), southerly air flows prevail in North

China.

It is evident that CAM5.1 can effectively capture the patterns of April–August monthly mean atmospheric circulation over East Asia. Furthermore, Fig. 3 illustrates that it can also depict the characteristics of 850-hPa averaged meridional wind and temperature pentad change. Thus, CAM5.1 is a good tool to simulate the effect of ULUC expansion on the EASTM.

3. Results

3.1 Impact of ULUC on surface climate

As shown in Fig. 4a, the surface air temperature increases in the concentrated plain area north of the Yangtze River and the Sichuan basin (30° – 40° N, 110° – 120° E); while in Figs. 4b and 4c, the increases in these regions for both intensity and range of surface air temperature never enhance (even shrinks in Figs. 4b and 4c), even with 1.5 and 2.5 times of increase in the urban land use. In all cases (Figs. 4a–c), North China experiences the most intensive increase of surface air temperature. However, summer surface air temperature increases more broadly and strongly in eastern China when the urban land use further increases (Figs. 4d–f). Meanwhile, the net surface radiation and sensible heat flux increase significantly, and the latent heat flux decreases significantly (figure omitted), which are favorable for an increase in surface air temperature.

The increase in surface air temperature owing to ULUC may further contribute to a change in air pressure and atmospheric circulation, under the urban expansion. The question arises, therefore, as to whether the increase in surface air temperature can have an effect on the onset and retreat of the EASTM and its northern boundary?

3.2 Onset and retreat of the EASTM under ULUC

3.2.1 Zonal LSTD

The onset of the EASTM depends on reversal of the zonal LSTD (Qi et al., 2008). The longitude of 120° E is always regarded as the boundary between land and sea in East Asia. In this study, the area with high zonal LSTD values is chosen as a critical area.

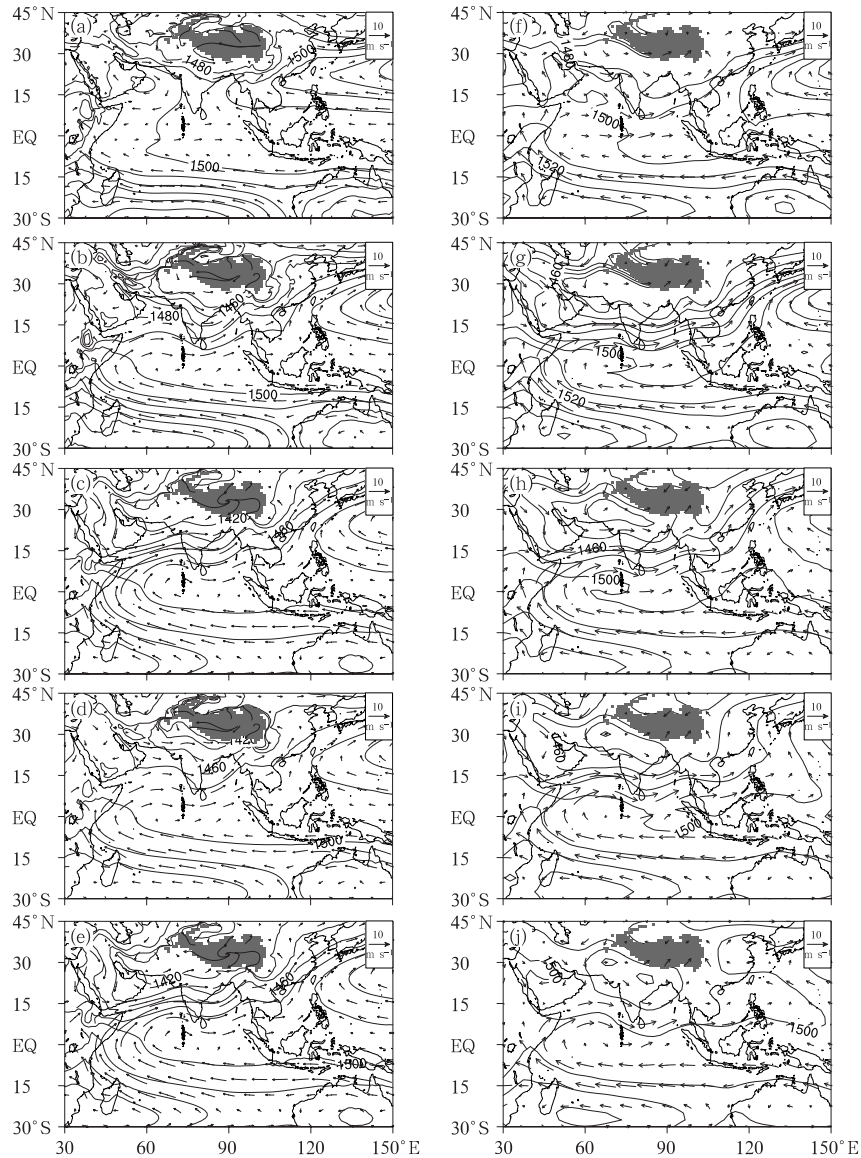


Fig. 2. Distributions of the monthly mean (April–August) 850-hPa wind field from (a–e) PRURB and (f–j) NCEP/NCAR reanalysis data (m s^{-1}) in (a, f) April, (b, g) May, (c, h) June, (d, i) July, and (e, j) August.

The areas 105° – 120°E and 130° – 150°E are selected to represent the East Asian land and the western Pacific sea areas, respectively. The zonal LSTD at 850 hPa from 27.5° to 32.5°N between the above two areas was plotted in Fig. 5, and a diagram was produced, showing the change in pentads of zonal temperature deviation from the 105° – 150°E mean (Fig. 6). The zonal LSTD indicates the thermal contrast between land and sea.

Figure 5 shows that in NOURB, the zonal LSTD turns negative in pentad 15 and turns positive in pen-

tad 53. In PRURB, meanwhile, the zonal LSTD turns negative and positive in pentads 16 and 54, respectively. Furthermore, in 1.5URB, 2.0URB, 3.0URB, 4.0URB, and 5.0URB, the zonal LSTD turns negative in pentads 17, 16, 19, 14, and 16, respectively, and reverses again in pentads 54, 55, 57, 53, and 53, respectively (Table 1). The effects of ULUC in eastern China on the zonal thermal difference in East Asia appear uncertain to some extent. However, in general, ULUC in eastern China may delay the reversal of the zonal thermal difference in East Asia.

According to the zonal temperature deviation, the ocean area in NOURB (Fig. 6a) before pentad 23 is a warm area. It then turns into a cold area after pentad 23 and in pentad 51, turns again to a warm area. For

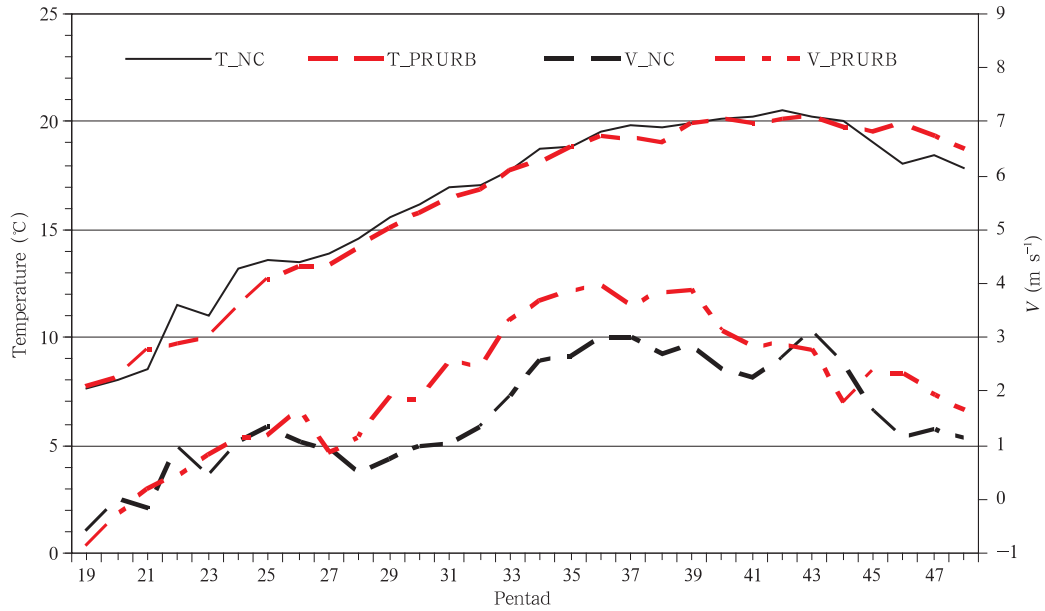


Fig. 3. Time series of averaged temperature ($^{\circ}\text{C}$) over $25^{\circ}\text{--}40^{\circ}\text{N}$, $110^{\circ}\text{--}120^{\circ}\text{E}$ and averaged meridional wind (m s^{-1}) over $25^{\circ}\text{--}40^{\circ}\text{N}$, $110^{\circ}\text{--}140^{\circ}\text{E}$ in PRURB and NCEP/NCAR reanalysis data at 850 hPa.

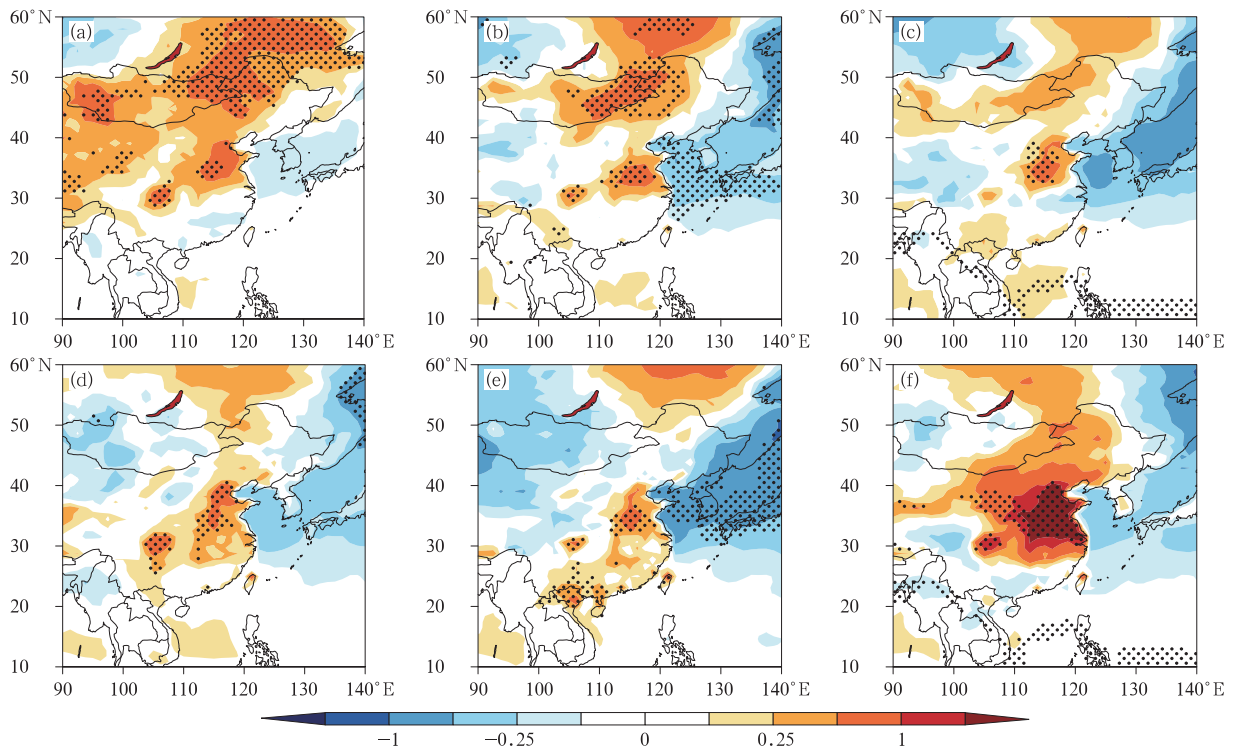


Fig. 4. Summer (June–July–August) mean changes in surface air temperature ($^{\circ}\text{C}$), with NOURB subtracted, from (a) PRURB, (b) 1.5URB, (c) 2.0URB, (d) 3.0URB, (e) 4.0URB, and (f) 5.0URB. Dots represent statistically significant changes at the 90% confidence level.

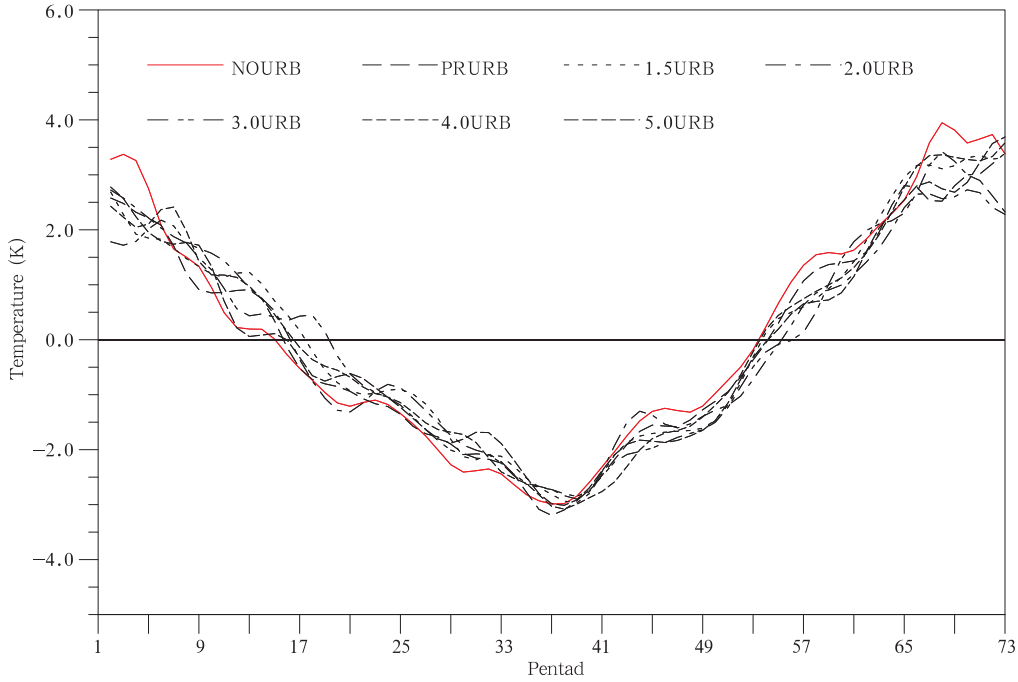


Fig. 5. Temporal evolutions of the zonal land-sea thermal contrast (K) at 850 hPa over 27.5° – 32.5° N. Zonal land-sea thermal contrast is defined as the average surface air temperature difference between the western Pacific Ocean (130° – 150° E) and the East Asian continent (105° – 120° E).

the land area in NOURB, it is a cold area before pentad 23, turns into a warm area after pentad 23, and turns again into a cold area in pentad 51. The ocean area in PRURB (Fig. 6b) is warm before pentad 25, cold from pentads 25 to 53, and then turns again into a warm area in pentad 53. In PRURB, the land is cold before pentad 25, turns into a warm area later on, and returns to a cold area after pentad 53. In PRURB, the difference between land and sea turns from positive to negative later than that in NOURB. Furthermore, its return to positive is also later. The other results with different levels of urban land cover fraction (Figs. 6b–f) also show the same features.

3.2.2 Onset and retreat of the EASTM

According to the definition in Section 2.3.1, Fig. 7 shows that in NOURB, the subtropical average meridional wind turns from north to south in pentad 18, meaning that the onset of the subtropical monsoon occurs in that pentad. The EASTM then retreats in pentad 54, when the southerly wind turns northerly. The onset of the EASTM is one pentad earlier in 4.0URB only; in the other experiments, the onset of the EASTM is delayed to pentad 21. In addition, for

the experiments with different levels of ULUC, the retreat of the EASTM is always delayed by two pentads (Table 1). The effects of ULUC on the onset and retreat of the EASTM appear uncertain to some extent. However, in general, ULUC delays the onset of the EASTM by three pentads, and the retreat by two pentads. The time that the average meridional wind reaches its peak is also delayed. The onset and retreat of the EASTM is basically consistent with the reversal of the thermal difference between the western Pacific and eastern China at 850 hPa.

The reversal of the meridional wind (i.e., the line of $V = 0$) involves a slow northerly tendency during the EASTM onset and a rapid southerly tendency when the EASTM retreats (He et al., 2007). Figure 8 indicates a slow northward tendency of the zero meridional wind line, corresponding to the onset of the EASTM. Figure 8a shows that in PRURB, the zero meridional wind line has a slower northward tendency than in NOURB, and that an abnormal northerly wind prevails in this area. This means that the turning of the meridional wind from north to south, and the northward movement of the zero meridional wind line,

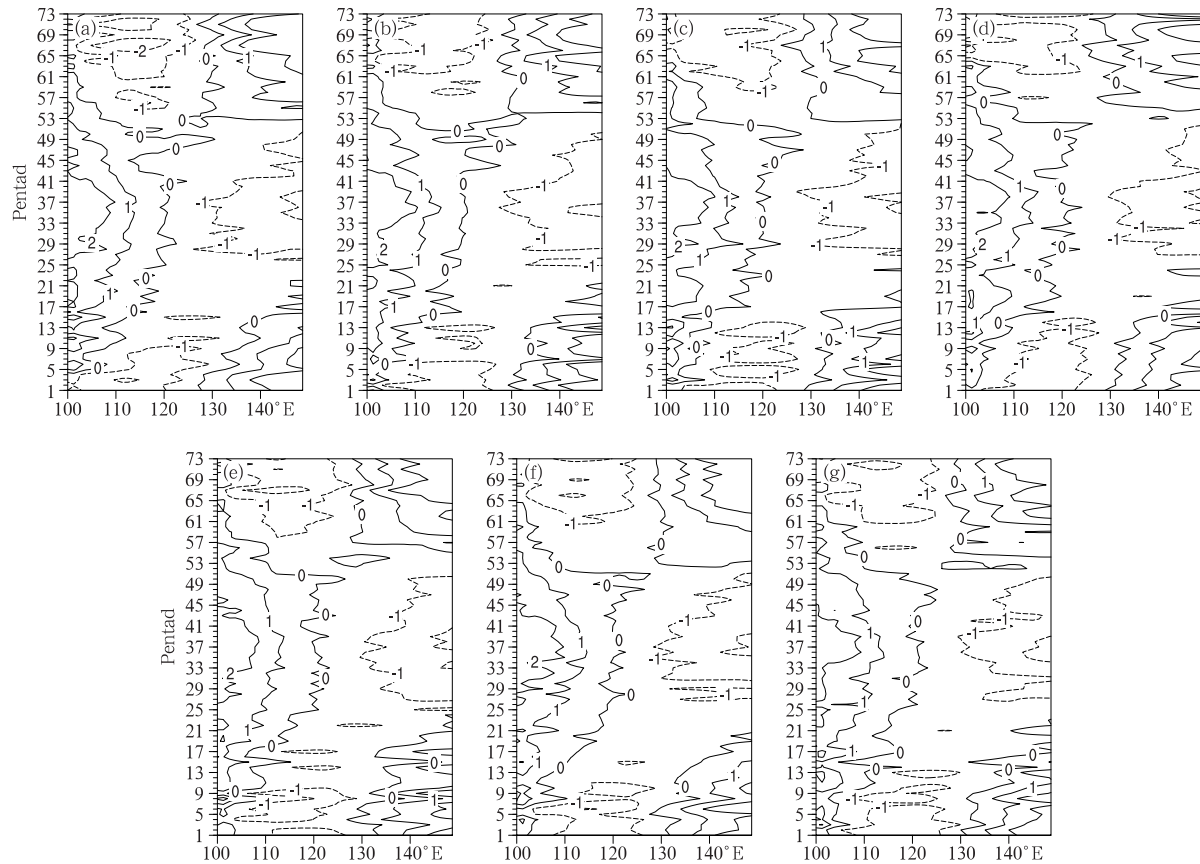


Fig. 6. Time-longitude evolutions of the surface air temperature deviation from the mean of 105° – 150° E (K) at 850 hPa over 27.5° – 32.5° N in (a) NOURB, (b) PRURB, (c) 1.5URB, (d) 2.0URB, (e) 3.0URB, (f) 4.0URB, and (g) 5.0URB.

Table 1. Time in pentad when the zonal LSTD changes signs in the seven experiments and associated EASTM onset and retreat dates (in pentad).

| Experiment | Zonal LSTD | | Onset date | Retreat date |
|------------|---------------------------|---------------------------|------------|--------------|
| | From positive to negative | From negative to positive | | |
| NOURB | 15 | 53 | 18 | 54 |
| PRURB | 16 | 54 | 21 | 55 |
| 1.5URB | 17 | 54 | 21 | 55 |
| 2.0URB | 16 | 55 | 22 | 56 |
| 3.0URB | 19 | 57 | 22 | 58 |
| 4.0URB | 15 | 53 | 17 | 56 |
| 5.0URB | 16 | 53 | 21 | 55 |
| Mean URB | 16 | 54 | 21 | 56 |

are slower/later than in NOURB. Figures 8b–f show that in the experiments with different levels of urban extension, the zero meridional wind line also possesses a slower northward tendency than in NOURB.

Similarly, in terms of the retreat of the EASTM (Fig. 9), the zero meridional wind line retreats southward quickly. Figure 9a shows that in PRURB, the

southerly wind retreats southward later, compared with that in NOURB, and an abnormal southerly wind prevails in this area. This means that in NOURB, the southerly wind retreats southward earlier, and turns from southerly to northerly earlier too. As indicated by Figs. 9b–f, under different levels of urban extension, the meridional wind always retreats southward

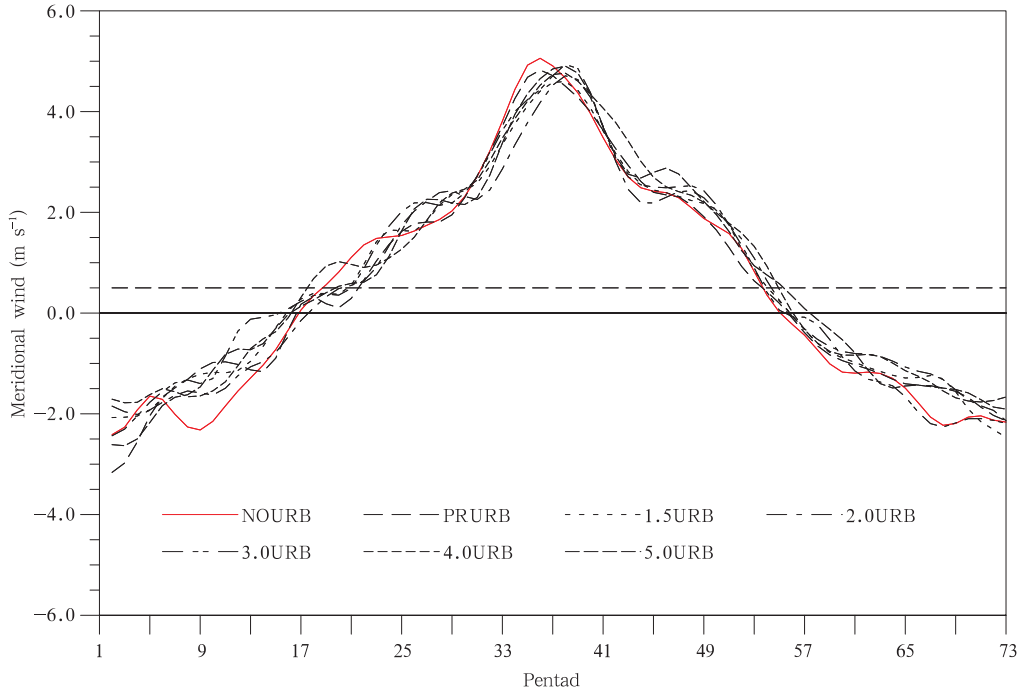


Fig. 7. Temporal evolutions of the meridional wind (m s^{-1}) averaged over the subtropical region (27.5° – 32.5°N , 110° – 140°E) at 850 hPa.

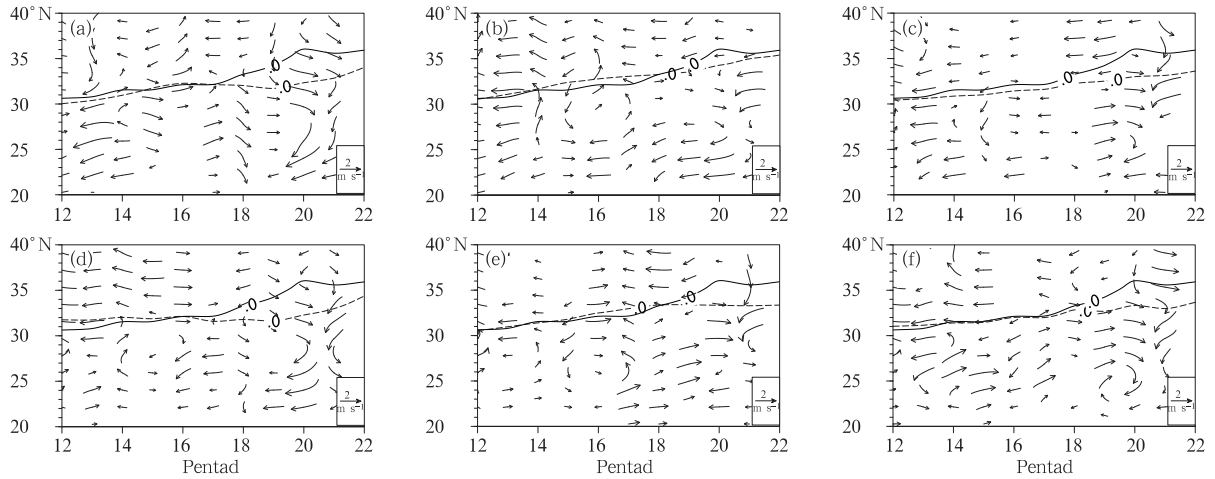


Fig. 8. Time–latitude cross-sections of the difference in the 850-hPa wind field (m s^{-1}) during the onset of the EASTM, with wind anomalies in NOURB subtracted from those in (a) PRURB, (b) 1.5URB, (c) 2.0URB, (d) 3.0URB, (e) 4.0URB, and (f) 5.0URB. Only the winds exceeding the 90% confidence level are shown. The zero meridional wind during the onset of the EASTM along 110° – 140°E in NOURB is shown by the solid lines and in other runs by dashed lines.

later. In conclusion, the thermal difference between land and sea turns negative later, and turns back positive later too, under the influence of ULUC. Furthermore, this also leads to a delay in the onset and retreat of the EASTM.

3.3 Effects of ULUC on the EASTM's northern boundary

3.3.1 General position of the EASTM

According to the definition in Section 2.3.2, Fig.

10 shows that the northern boundary of the East Asian summer monsoon appears most northerly at 48°N and most southerly at 32.5°N in 1998 and 1999, respectively. The variation in the most northerly location of the northern boundary of the EASTM has a trend of $-0.24^{\circ}\text{ yr}^{-1}$ (dashed line in Fig. 10), statistically significant at the 95% confidence level. This means that the northern boundary of the East Asian summer monsoon was located more southward during 1993–2007. In fact, the development of urban areas was very quick during this period of time. This may be one of the

reasons for the general southward movement of the EASTM.

3.3.2 Northern boundary of the EASTM

According to the definition in Section 2.3.2, Fig. 11a shows that in NOURB, the northern boundary of the EASTM appears firstly in pentad 25, and is located near 17°N . In pentad 31, it moves northward to the lower-mid reaches of the Yangtze River, and then continues to move to North China. In pentad 39, it is located near 47°N , and then retreats southward and decays near 38°N in pentad 45. In PRURB

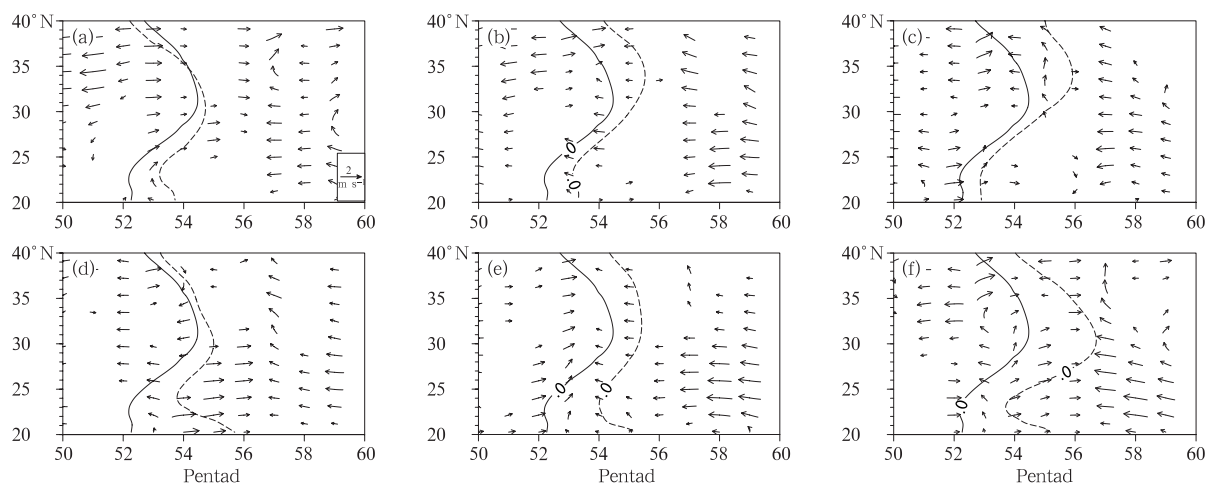


Fig. 9. As in Fig. 8, but during the retreat of the EASTM.

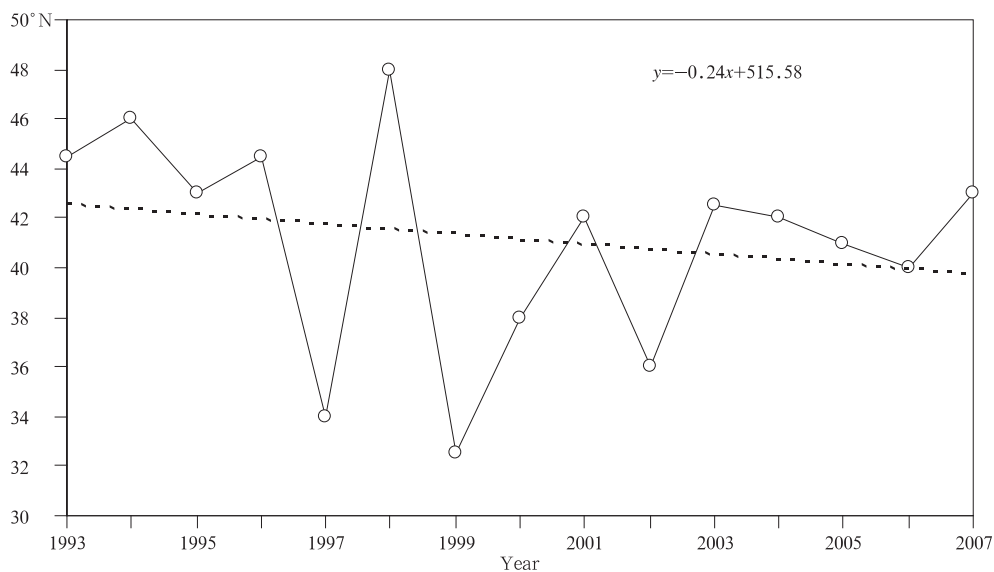


Fig. 10. Time series of the most northerly location of the northern boundary of the EASTM over 110° – 120°E from 1993 to 2007, based on NCEP/NCAR reanalysis data.

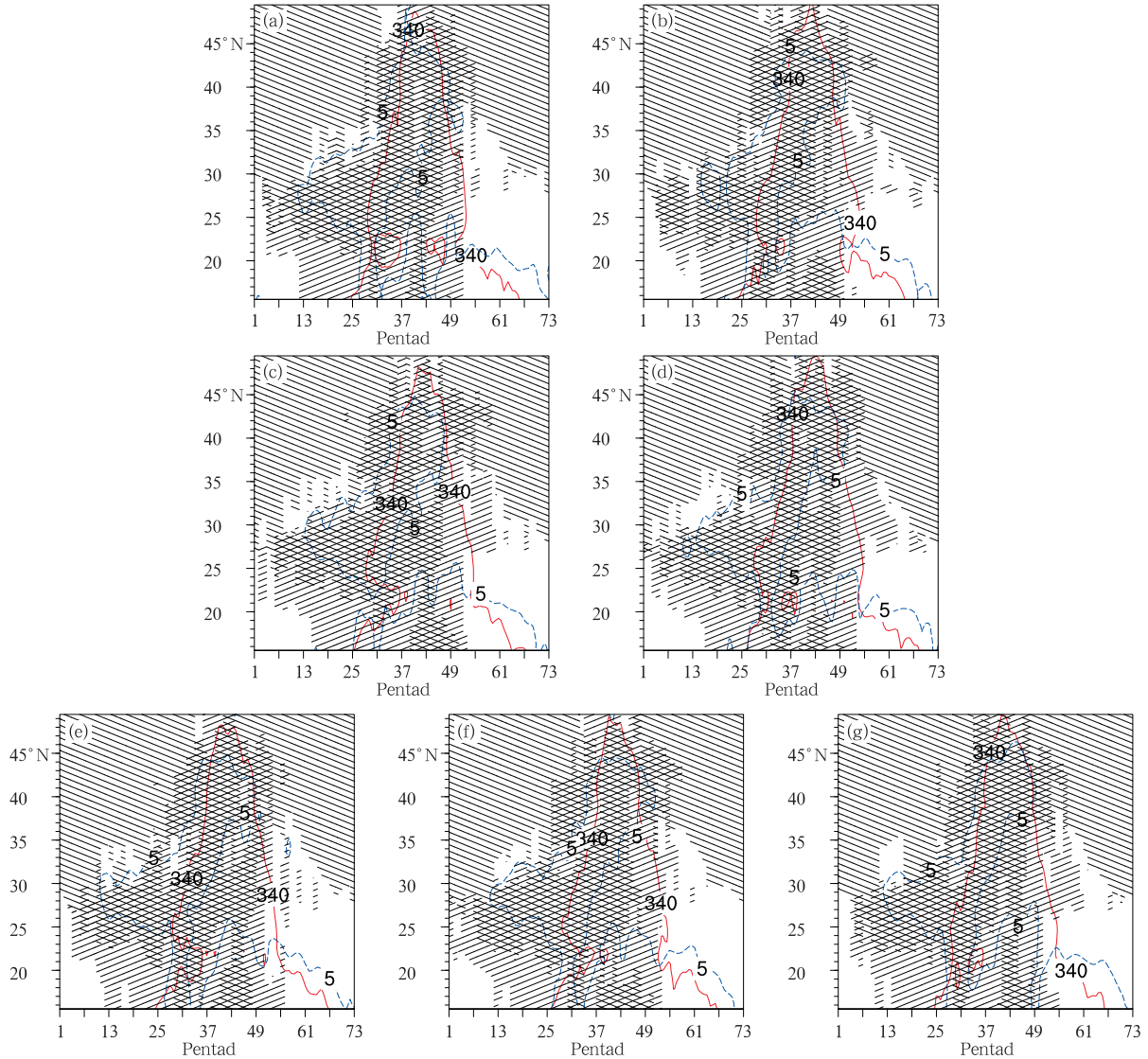


Fig. 11. Evolutions of the northern boundary ($^{\circ}$ N) of the EASTM along 110° – 120° E in (a) NOURB, (b) PRURB, (c) 1.5URB, (d) 2.0URB, (e) 3.0URB, (f) 4.0URB, and (g) 5.0URB. Hatched areas denote southwesterlies, right slanted lines mean westerlies, and left slanted lines mean southerlies. Red lines denote $\theta_{se}=340$ K, and blue dashed lines denote pentad precipitation of 4 mm day^{-1} .

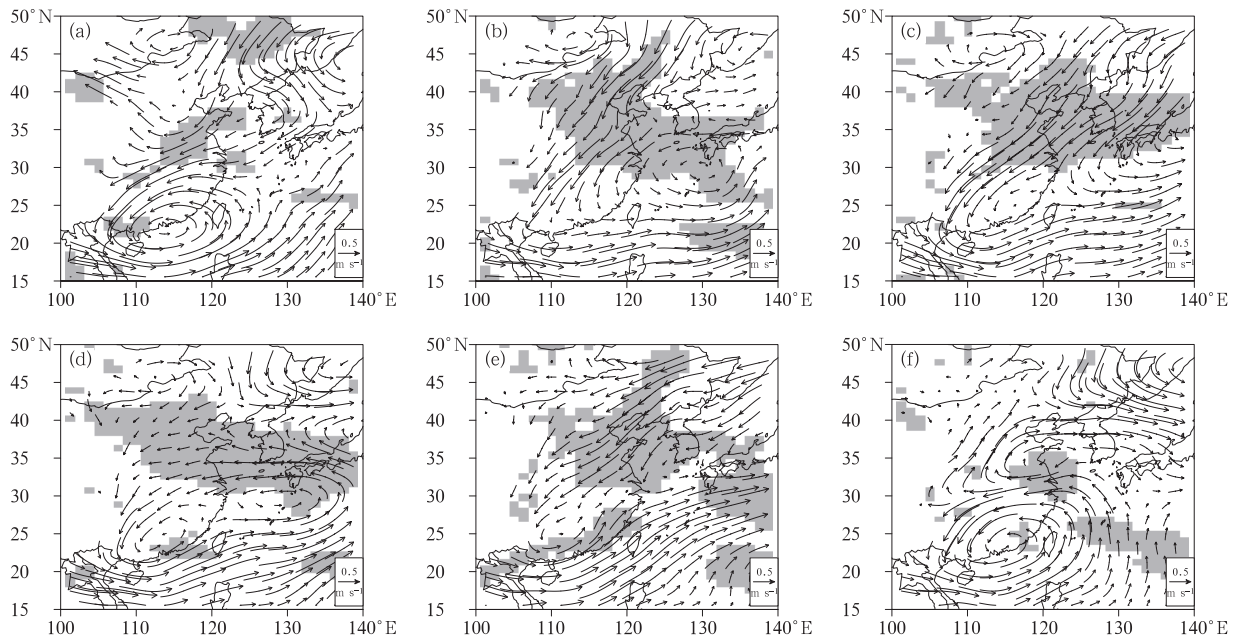
(Fig. 11b), the northern boundary of the EASTM appears firstly in pentad 25, near 18° N. Then, it moves slowly northward to the lower–mid reaches of the Yangtze River in pentad 31, after which it pushes northward quickly and reaches 44° N in pentad 41. Finally, it decays near 39° N in pentad 46. However, in 1.5URB, 2.0URB, 3.0URB, 4.0URB, and 5.0URB (Figs. 11c–g), the most northerly location of the northern boundary of the EASTM appears at 45° , 45° ,

44° , 44° , and 46° N, respectively (Table 2). Therefore, the effects of urban expansion may lead to a southward movement of the northern boundary of the EASTM.

Furthermore, based on the difference in the wind field between NOURB and those different urban extension runs (Fig. 12), it is apparent that from North China to the mid-lower reaches of the Yangtze River, northerly flows prevail, and the climatological warm and wet southerly is weakened. This may be the

Table 2. The most northerly location ($^{\circ}\text{N}$) of the northern boundary of the EASTM in the seven experiments

| Location ($^{\circ}\text{N}$) | Experiment | | | | | | | |
|---------------------------------|------------|-------|--------|--------|--------|--------|--------|----------|
| | NOURB | PRURB | 1.5URB | 2.0URB | 3.0URB | 4.0URB | 5.0URB | Mean URB |
| | 47 | 44 | 45 | 45 | 44 | 44 | 46 | 45 |

**Fig. 12.** Summer (June–July–August) mean changes in wind (m s^{-1}) at 850 hPa over East Asia, with the wind anomalies in NOURB subtracted from those in (a) PRURB, (b) 1.5URB, (c) 2.0URB, (d) 3.0URB, (e) 4.0URB, and (f) 5.0URB. Shaded areas represent the statistically significant changes at the 90% confidence level.

reason for the slower northward advancement of the EASTM and a more southward location of its northern boundary.

In conclusion, ULUC causes the land surface air temperature in eastern China in summer to rise, and the associated wind anomalies to be unfavorable for the northerly advancement of the EASTM. Ultimately, this leads to a more southward location of the northern boundary of the EASTM. The observational fact also reveals that the northern boundary of the EASTM has withdrawn southward since the 2000s, coinciding with the rapid increase in urban land-use that has taken place during this period of time. The experiments in this study illustrate that urban expansion is one of the reasons for the southward retreat of the EASTM and its northern boundary.

4. Conclusions and discussion

Based on the experiments, we conducted using the

high-resolution CAM5.1, the impact of ULUC in eastern China on the onset and retreat of the EASTM and its northern boundary, as well as the possible mechanism involved, was investigated in this study. The results are summarized as follows.

(1) Owing to development of large-scale urban clusters in eastern China, alterations in the surface parameters (e.g., surface temperature, albedo, and roughness) and surface energy balance characteristics have taken place. The surface absorbs more solar radiation; net radiation, sensible heat flux, and surface temperature increase, and latent heat flux decreases. Comparison of the urban expansion runs with the NOURB run shows that the change in LSTD caused by ULUC contributes to a delay in the time when LSTD converts from positive to negative, and vice versa. As a result, the onset date and end date of the EASTM are delayed.

(2) The rise in surface air temperature caused by

ULUC leads to formation of abnormal northerly air flows, which may cause the EASTM to move northward slowly. This may also contribute to a more southern position of the EASTM's northern boundary.

It is important to highlight that, in this study, numerical simulations were used to investigate the effect of ULUC. In reality, aerosol emissions and greenhouse gases resulting from urbanization can also affect climate and weather. Furthermore, the influence of urbanization presented in the air-sea coupled model simulations may differ from that in atmospheric models driven by prescribed SST (Chung and Seinfeld, 2005; Wang et al., 2005; Lau and Kim, 2006). Thus, further investigation is required for a more comprehensive understanding of the large-scale urbanization effects on climate change.

Acknowledgments. We thank the editor and three anonymous reviewers for their valuable comments and suggestions.

REFERENCES

- Ao Xiangyu, Ren Xuejuan, Tang Jianping, et al., 2012: Simulation study of urbanization effects on summer daily precipitation over the Yangtze River Delta. *Scientia Meteor. Sinica*, **31**, 451–459. (in Chinese)
- Chen, H. S., and Y. Zhang, 2013: Sensitivity experiments of impacts of large-scale urbanization in East China on East Asian winter monsoon. *Chin. Sci. Bull.*, **58**, 809–815.
- Chen, H. S., Y. Zhang, M. Yu, et al., 2015: Large-scale urbanization effects on eastern Asian summer monsoon circulation and climate. *Climate Dyn.*, doi:10.1007/s00382-015-2827-3.
- Chung, S. H., and J. H. Seinfeld, 2005: Climate response of direct radiative forcing of anthropogenic black carbon. *J. Geophys. Res.*, **110**, doi: 10.1029/2004JD005441.
- Christidis, N., P. A. Stott, G. C. Hegerl, et al., 2013: The role of land use change in the recent warming of daily extreme temperatures. *Geophys. Res. Lett.*, **40**, 589–594.
- Deng Jiechun and Xu Haiming, 2014: Possible impact of urbanization extension over eastern China on spring climate in East Asia. *J. Nanjing. Univ. (Nat. Sci. Ed.)*, **50**, 748–758. (in Chinese)
- Deng Jiechun, Xu Haiming, Ma Hongyun, et al., 2014a: A numerical study of the effect of anthropogenic aerosols over the eastern China on East Asian summer monsoon onset and its northward advancement. *J. Trop. Meteor.*, **30**, 952–962. (in Chinese)
- Deng Jiechun, Xu Haiming, Ma Hongyun, et al., 2014b: Numerical study of the effect of anthropogenic aerosols on spring persistent rain over eastern China. *J. Meteor. Res.*, **28**, 341–353.
- Ding, Y. H., Y. J. Liu, Y. F. Song, et al., 2015: From MONEX to the global monsoon: A review of monsoon system research. *Adv. Atmos. Sci.*, **32**, 10–31.
- He Jinhai, Qi Li, Wei Jin, et al., 2007: Reinvestigations on the East Asian subtropical monsoon and tropical monsoon. *Chinese J. Atmos. Sci.*, **31**, 1257–1265. (in Chinese)
- He Jinhai, Zhao Ping, Zhu Congwen, et al., 2008: Discussion of some problems as to the East Asian subtropical monsoon. *Acta Meteor. Sinica*, **22**, 419–434.
- Hu Haoran and Qian Weihong, 2007: Acknowledgment of the north boundary of Asian summer monsoon. *Progress in Natural Science*, **17**, 57–65. (in Chinese)
- Hurrell, J. W., J. J. Hack, D. Shea, et al., 2008: A new sea surface temperature and sea ice boundary dataset for the Community Atmosphere Model. *J. Climate*, **21**, 5145–5153.
- IPCC, 2013: Climate Change 2013: The Physical Science Basis. *Contribution of Working Group I to the Fifth Assessment Report of the Intergovernmental Panel on Climate Change*, Stocker, T. F., D. Qin, G. K. Plattner, et al., Eds., Cambridge University Press, Cambridge, United Kingdom and New York, NY, USA, 649–740.
- Jiang Zhihong, He Jinhai, Li Jianping, et al., 2006: Northerly advancement characteristics of the East Asian summer monsoon with its interdecadal variations. *Acta Geographica Sinica*, **61**, 675–686. (in Chinese)
- Kalnay, E., M. Kanamitsu, R. Kistler, et al., 1996: The NCEP/NCAR 40-year reanalysis project. *Bull. Amer. Meteor. Soc.*, **77**, 437–471.
- Kalnay, E., and M. Cai, 2003: Impact of urbanization and land-use change on climate. *Nature*, **423**, 528–531.
- Lau, K. M., and K. M. Kim, 2006: Observational relationships between aerosol and Asian monsoon rainfall, and circulation. *Geophys. Res. Lett.*, **33**, doi: 10.1029/2006GL027546.

- Li Dongliang, Shao Pengcheng, Wang Hui, et al., 2013a: Advances in research of the north boundary belt of East Asian subtropical summer monsoon in China. *Plateau Meteor.*, **32**, 305–314. (in Chinese)
- Li Dongliang, Shao Pengcheng, and Wang Hui, 2013b: The position variations of the north boundary of East Asian subtropical summer monsoon during 1951–2009. *J. Desert Res.*, **33**, 1511–1519. (in Chinese)
- Li Xin, Yang Xiuqun, Tang Jianping, et al., 2011: Multiple urban heat islands and surface energy balance during summer in Yangtze River Delta city cluster region simulated with WRF/NCAR. *Scientia Meteor. Sinica.*, **31**, 441–450. (in Chinese)
- Ma Hongyun, Xue Jiaqing, Jiang Zhihong, et al., 2014: A numerical study of the impact of urban land-use change over eastern China on South China Sea monsoon onset. *J. Nanjing Univ. (Nat. Sci.)*, **6**, 737–747. (in Chinese)
- Ma Hongyun, Jiang Zhihong, Song Jie, et al., 2015: Effects of urban land-use change in East China on the East Asian summer monsoon based on the CAM5.1 model. *Climate Dyn.*, doi 10.1007/s00382-015-2745-4.
- Neale, R. B., C. C. Chen, A. Gettelman, et al., 2010: Description of the NCAR community atmosphere model (CAM5.0). NCAR Technical Note, NCAR/TN-486+STR. 274 pp.
- Oleson, K. W., D. M. Lawrence, G. B. Bonan, et al., 2010: Technical description of version 4.0 of the community land model (CLM). *Geophys. Res. Lett.*, **37**, 256–265.
- Oleson, K. W., G. B. Bonan, J. Feddema, et al., 2008: An urban parameterization for a global climate model. Part I: Formulation and evaluation for two cities. *J. Appl. Meteor. Climatol.*, **47**, 1038–1060.
- Oleson, K. W., G. B. Bonan, J. Feddema, et al., 2015: Technical description of an urban parameterization for the Community Land Model (CLMU). Tech Note NCAR/TN, **37**, 256–265.
- Pitman, A. J., N. deNoblet-Ducoudré, F. B. Avila, et al., 2012: Effects of land cover change on temperature and rainfall extremes in multi-model ensemble simulations. *Earth Syst. Dynam.*, **3**, 597–641.
- Qi Li, He Jinhai, Zhang Zuqiang, et al., 2008: Seasonal transformation of zonal sea-land thermal difference and the East Asian subtropical monsoon circulation. *Chin. Sci. Bull.*, **66**, 940–954. (in Chinese)
- Tang Xu, Qian Weihong, and Liang Ping, 2006: Climatic features of the boundaries for the East Asian summer monsoon. *Plateau Meteor.*, **25**, 375–381. (in Chinese)
- The National Bureau of Statistics, 2014: *China City Statistical Yearbook*. China Statistics Press, Beijing. (in Chinese)
- Wang, B., and Lin Ho, 2002: Rainy season of the Asian-Pacific summer monsoon. *J. Climate*, **15**, 386–398.
- Wang, B., Lin Ho, Y. S. Zhang, et al., 2004: Definition of South China Sea monsoon onset and commencement of the East Asian summer monsoon. *J. Climate*, **17**, 699–710.
- Wang, B., Q. H. Ding, X. H. Fu, et al., 2005: Fundamental challenge in simulation and prediction of summer monsoon rainfall. *Geophys. Res. Lett.*, **32**, L15711.
- Wang Dongdong, Zhu Bin, Jiang Zhihong, et al., 2014: Direct effect of sulfate aerosols on the process of the East Asian subtropical monsoon. *Chinese J. Atmos. Sci.*, **38**, 897–908. (in Chinese)
- Wang, H. J., 2001: The weakening of the Asian monsoon circulation after the end of 1970s. *Adv. Atmos. Sci.*, **18**, 376–386.
- Wang Huijun and Fan Ke, 2013: Recent changes in the East Asian monsoon. *Chinese J. Atmos. Sci.*, **37**, 313–318. (in Chinese)
- Wu Kaia and Yang Xiuqun, 2013: Urbanization and heterogeneous surface warming in eastern China. *Chin. Sci. Bull.*, **58**, 1363–1373.
- Zhang, C. L., F. Chen, S. G. Miao, et al., 2009: Impacts of urban expansion and future green planting on summer precipitation in the Beijing metropolitan area. *J. Geophys. Res.*, **114**, doi: 10.1029/2008JD010328.
- Zhang Lu, Yang Xiuqun, Tang Jianping, et al., 2011: Simulation of urban heat island effect and its impact on atmospheric boundary layer structure over Yangtze River Delta region in summer. *Scientia Meteor. Sinica*, **31**, 431–440. (in Chinese)
- Zhao Ping, Zhou Xiuji, Chen Longxun, et al., 2009: Characteristics of subtropical monsoon and rainfall over eastern China and western North Pacific. *Acta Meteor. Sinica*, **23**, 649–665.
- Zhu, Q. G., J. H. He, and P. X. Wang, 1986: A study of circulation differences between East-Asian and Indian summer monsoons with their interaction. *Adv. Atmos. Sci.*, **3**, 466–477.